

## Supporting Information

### Bandgap Engineering of Coal-Derived Graphene Quantum Dots

*Ruquan Ye,<sup>†</sup> Zhiwei Peng,<sup>†</sup> Andrew Metzger,<sup>†</sup> Jian Lin,<sup>‡,§,±</sup> Jason A. Mann,<sup>†</sup> Kewei Huang,<sup>†</sup>*

*Changsheng Xiang,<sup>†</sup> Xiujun Fan,<sup>‡,§,†</sup> Errol L. G. Samuel,<sup>†</sup> Lawrence B. Alemany,<sup>†,§,#</sup> Angel A.*

*Martí<sup>\*,†,‡,§</sup> and James M. Tour<sup>\*,†,‡,§</sup>*

*<sup>†</sup>Department of Chemistry, <sup>‡</sup>Department of Materials Science and NanoEngineering,*

*<sup>§</sup>Smalley Institute for Nanoscale Science and Technology, <sup>#</sup>Shared Equipment Authority, Rice*

*University, 6100 Main Street, Houston, Texas 77005, USA. <sup>±</sup>Department of Mechanical &*

*Aerospace Engineering, University of Missouri-Columbia Columbia, Missouri 65211, USA,*

*<sup>†</sup>College of Electronic Information and Control Engineering, Beijing University of Technology,*

*Beijing 100124, China*

*E-mail: [amarti@rice.edu](mailto:amarti@rice.edu); [tour@rice.edu](mailto:tour@rice.edu)*

#### Table of Contents

1. Experimental Procedure
2. Equations
3. Supplementary Figures.

#### 1. Experimental Procedure

**Materials.** Anthracite (Fisher Scientific, catalogue number S98806), bituminous coal (Fisher Scientific, catalogue number S98809), graphite (Sigma-Aldrich, catalogue number 332461, B150mm flakes), H<sub>2</sub>SO<sub>4</sub> (95–98%, Sigma-Aldrich), and HNO<sub>3</sub> (70%, Sigma-Aldrich) were used as received unless noted otherwise. Polytetrafluoroethylene membranes (Sartorius, lot number 11806-47-N) and dialysis bags (Membrane Filtration Products, Inc. Product number 1-0150-45) were used to purify the GQDs. The cross-flow ultrafiltration instrument was a Spectrum Labs *Krosflo*, Research III TFF System.

**Preparation of GQDs for cross-flow ultrafiltration.** In a typical procedure, 6 g of anthracite was dispersed in a mixed solvent of 225 mL sulfuric acid and 75 mL nitric acid. The solution was sonicated (Cole Parmer, model 08849 - 00) for 2 h and then heated at 100 °C for 1 d. After the thermal oxidation, a clear brown-red solution resulted. The solution was then cooled in an ice-water bath and diluted 3× with DI water. After that, the solution was dialyzed in 1000 Dalton dialysis bag against DI water for 3 d.

**Separation of GQDs by cross-flow ultrafiltration.** As illustrated in Figure 1b, the as-prepared GQDs are separated using cross-flow ultrafiltration with 3, 10 and 30 kilo Dalton (kD) membranes at ~ 1 atm transmembrane pressure TMP. As the pore size and TMP increased, the permeability of GQDs increased. Thus, by exploiting appropriate membrane size and TMP values, GQDs with different size distribution were obtained. The membrane was changed when the permeate turned from brown to colorless. Each separation batch took 1 to 2 h.

**Preparation of GQDs at varying temperatures.** In a typical procedure, 3 g of anthracite was dispersed in a mixed solvent of 225 mL sulfuric acid and 75 mL nitric acid. The solution was sonicated (Cole Parmer, model 08849-00) for 2 h and then heated at different temperatures (50 to 150 °C) for 1 d. After the thermal oxidation, a clear brown-red solution resulted. The solution was then cooled in an ice-water bath and diluted 3× with DI water. After that, the solution was dialyzed in 1000 Dalton dialysis bag against DI water for 3 d.

**Improving the quantum yield by NaOH treatment.**

In a typical procedure, a 15 mL solution containing 1 mg/mL GQDs in 0.2 M aqueous NaOH was prepared, transferred to a sealed Teflon autoclave and heated to 180 °C for 1 d. After cooling to room temperature, the solution was transferred to a 1000 Dalton dialysis bag and was dialyzed against DI water for 3 d.

**Improving the quantum yield by Na<sub>2</sub>S treatment.**

In a typical procedure, a 15 mL aqueous solution containing 1 mg/mL GQDs in 1 M Na<sub>2</sub>S was prepared in a round-bottom flask. The solution was heated to 100 °C under nitrogen for 1 d. After cooling to room temperature, the solution was transferred to a 1000 Dalton dialysis bag and was dialyzed against DI water for 3 d.

**Sample Characterization.** The transmission electron microscopy (TEM) were taken using a 2100 F field emission gun TEM with GQDs directly transferred onto a C-flat TEM grid. Dynamic light scattering was performed on a Malvern Zen 3600 Zetasizer with refractive index of 2 at 25 °C. X-ray photoelectron spectroscopy (XPS) spectra were measured on a PHI Quantera

SXM scanning X-ray microprobe with a 45° take-off angle and 100 µm beam size; the pass energy for surveys was 140 and 26 eV for high-resolution scans. A 2 nm Au layer was sputtered (Denton Desk V Sputter system) on the sample surface before scanning. Raman microscopy was performed with a Renishaw Raman microscope using 514 nm laser excitation at room temperature. Mass spectrometry was conducted on a Bruker Autoflex MALDI ToF instrument. Ultraviolet–visible (UV) spectra were recorded on a Shimadzu UV-2450 ultraviolet–visible spectrophotometer. Steady-state spectra were obtained in a HORIBA JovinYvon Fluorolog 3. Solid state FTIR spectra were obtained on a Nicolet FTIR Microscope with an MCT/B detector. <sup>13</sup>C Nuclear magnetic resonance (NMR) was performed on a Bruker Avance III 4.7 T spectrometer (50.3 MHz <sup>13</sup>C, 200.1 MHz <sup>1</sup>H) with a standard broadband MAS probe designed for 4 mm rotors. Direct <sup>13</sup>C pulse spectra were obtained with 12 kHz MAS, a 90° pulse, 20.5 ms FID, 10 s relaxation delay, and differing number of scans (1440 for GQDs-S4.5, 1600 for GQDs-S16, 3400 for GQDs-S41, 3280 for GQDs-S70, 9024 for GQDs-T150-7.6, 16928 for GQDs-T130-25, 8096 for GQDs-T110-27 and 6328 for GQDs-T50-54), with each FID processed with 50 Hz (1 ppm) of line broadening. <sup>1</sup>H-<sup>13</sup>C CP spectra were obtained with 7.6 kHz MAS, a 1 ms contact time, 32.8 ms FID, 5 s relaxation delay, and differing number of scans (10600 for each of GQDs-S4.5, GQDs-S41, GQDs-S70 and 10400 for GQDs-S16, 30632 for GQDs-T150-7.6, 32600 for GQDs-T130-25, 14000 for GQDs-T110-27, and 17000 for GQDs-T50-54), with each FID processed with 50 Hz of line broadening. More scans were taken for GQDs-T150-7.6 and GQDs-T130-25 to compensate for the limited amount of sample

available.

## 2. Equations

### Transmembrane pressure

$$\text{TMP} = \frac{P_F + P_R}{2} - P_P$$

Where  $P_F$ ,  $P_R$ ,  $P_P$  are the pressure at feed, retentate and permeate, respectively. The TMP value used in the cross-flow filtration was kept constant at ~1 atm.

### Quantum yield calculation

$$\Phi_i = \Phi_r \frac{I_i(1 - 10^{-A_r})n_i^2}{I_r(1 - 10^{-A_i})n_r^2}$$

Where  $\Phi_i$ ,  $\Phi_r$  are the quantum yield of samples and reference, respectively. The integrated intensities (area) of sample and reference are  $I_i$  and  $I_r$ , respectively;  $A_i$  and  $A_r$  are the absorbance,  $n_i$  and  $n_r$  are the refractive indices of the samples and reference solution, respectively.

### XRD d-spacing calculation

$$2d\sin(\theta) = n\lambda$$

where  $d$  is the d-spacing,  $\theta$  is the XRD peak,  $\lambda$  is the X-ray wavelength (Copper source,  $\lambda=0.154059$  nm). This equation can be used to calculate the d-spacing of the (002) crystalline structure of anthracite and graphite.

### 3. Supplementary Figures

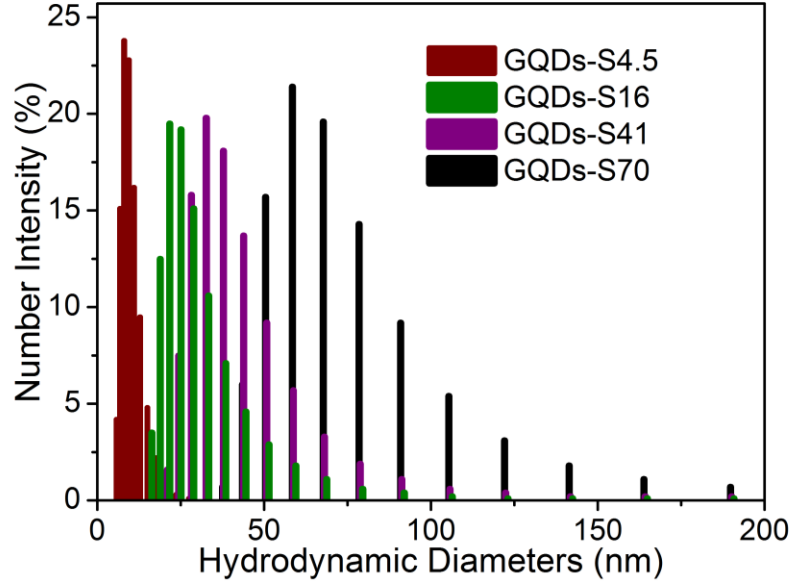


**Figure S1.** Hydrodynamic diameters of GQDs at different sizes obtained from dynamic light scattering. The legend sizes are listed so as to be consistent with the TEM legend, but the actual DLS recorded average sizes are  $10 \pm 2.5$ ,  $27 \pm 7.9$ ,  $41 \pm 11$  and  $76 \pm 18$  nm, respectively. The fitting was using lognormal function:

$$y = y_c + \frac{1}{x\sqrt{2\pi}\sigma} e^{-\frac{(\ln x - \mu)^2}{2\sigma^2}}$$

where

$$\text{Mean} = e^{\mu + \sigma^2/2}$$

$$\text{Standard Deviation} = \sqrt{e^{\sigma^2} - 1} e^{\mu + \sigma^2/2}$$

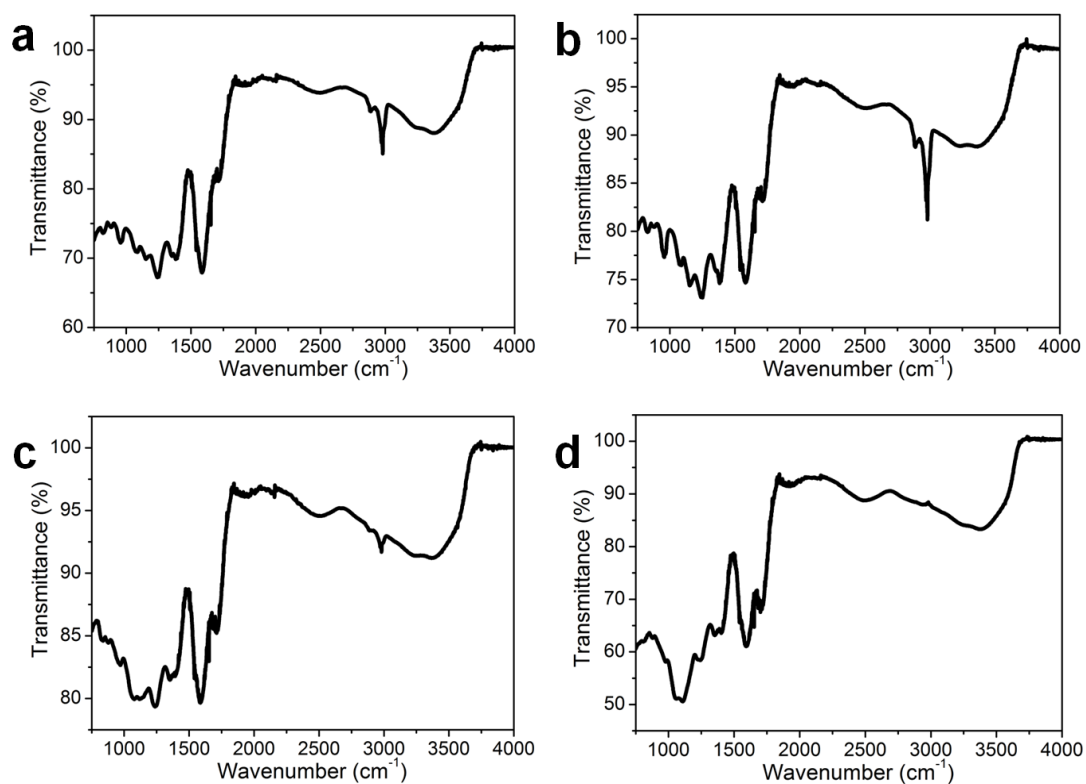


**Figure S2.** Solid state FTIR spectra of (a) GQDs-S4.5, (b) GQDs-S16, (c) GQDs-S41 and (d) GQDs-S70.

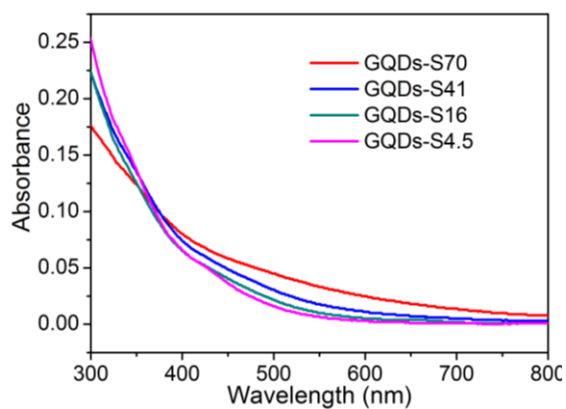


**Figure S3.** UV-Vis absorption of GQDs-S4.5, GQDs-S16, GQDs-S41 and GQDs-S70.

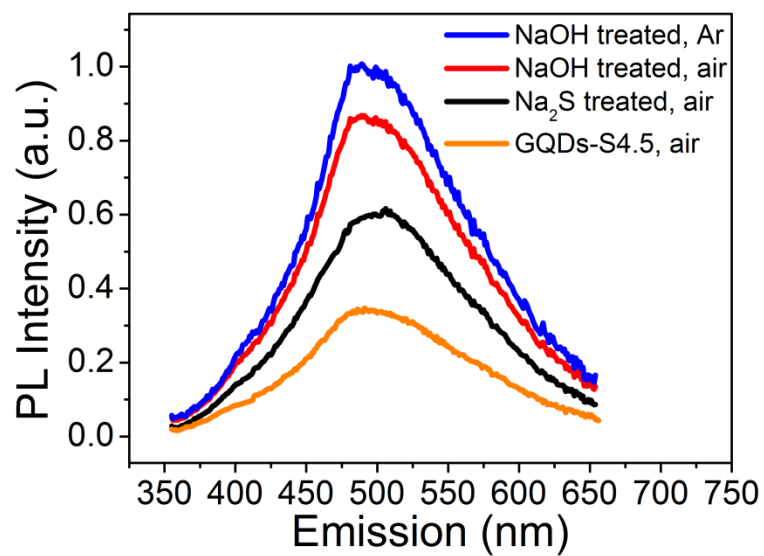


**Figure S4.** Photoluminescence of GQDs-S4.5 before and after NaOH or Na<sub>2</sub>S treatment.

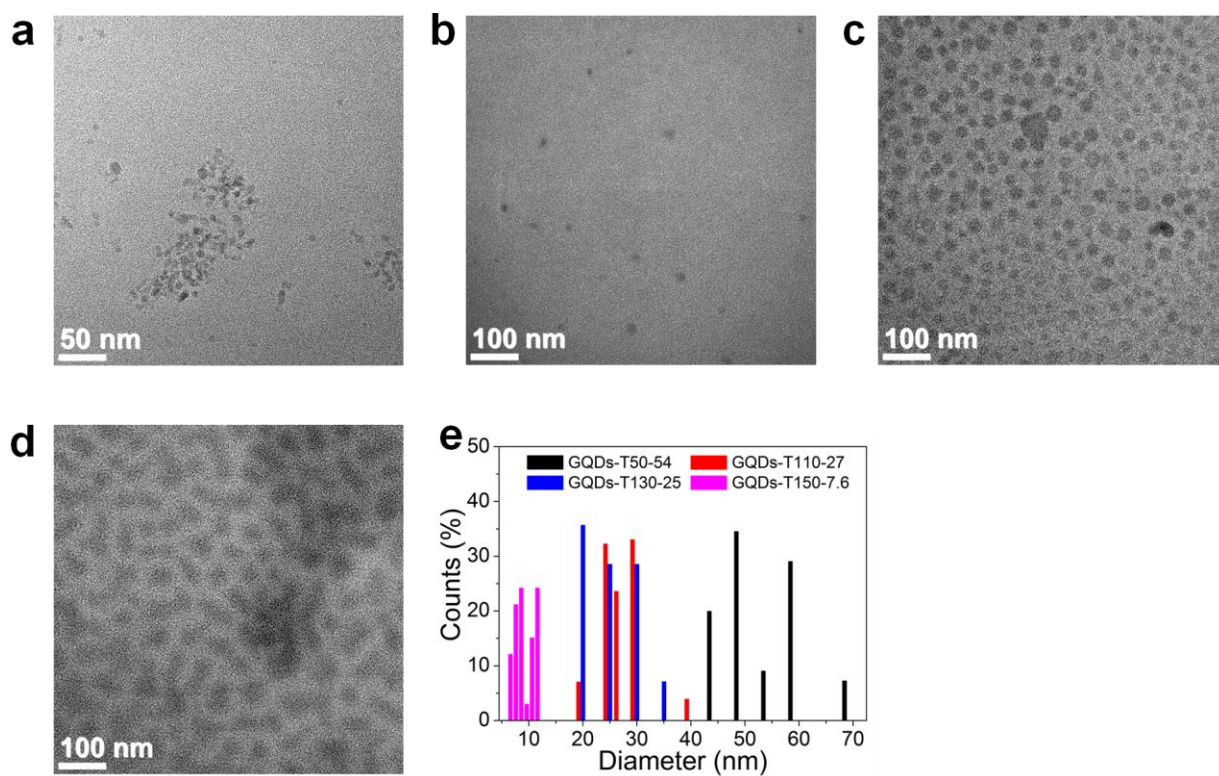


**Figure S5.** TEM images of GQDs synthesized at different temperatures (a) GQDs-T150-7.6, (b)



GQDs-T130-25, (c) GQDs-T110-27 and (d) GQDs-T50-54. The corresponding average diameters from the TEM images are  $7.6 \pm 1.8$ ,  $25 \pm 5.0$ ,  $27 \pm 3.8$  and  $54 \pm 7.2$  nm, respectively. (e) Summary of size distributions of GQDs from (a) to (d).

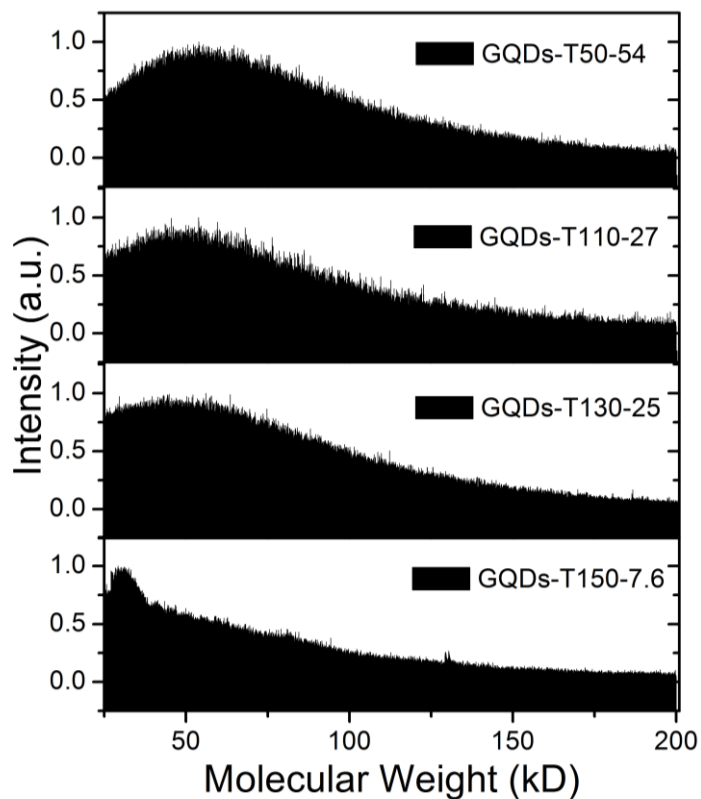


**Figure S6.** MALDI-MS of GQDs synthesized at different temperatures. The average diameter of the GQDs was  $54 \pm 7.2$ ,  $27 \pm 3.8$ ,  $25 \pm 5.0$ , and  $7.6 \pm 1.8$  nm as the synthesis temperature rose from 50 to 150 °C (from top to bottom in the Figure). The corresponding molecular weights of the GQDs peaks were 60, 49, 44 and 27 kD, respectively.

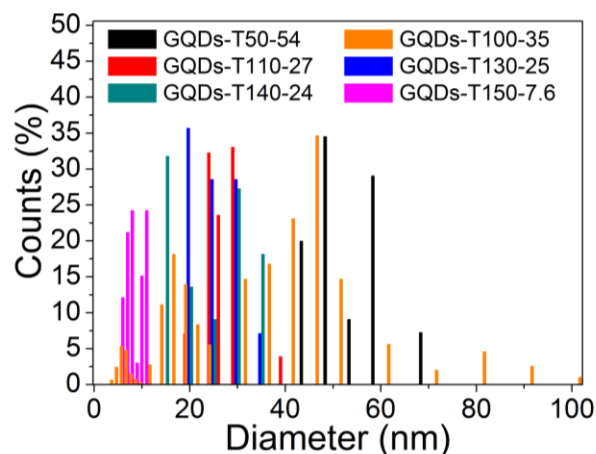


**Figure S7.** A composite plot of Figure 1g and Figure S5e. GQDs-T100-35 is composed of GQDs-S4.5, GQDs-S16, GQDs-S41 and GQDs-S70. Comparing all the GQDs synthesized at different temperature, GQDs-T100-35 contains particles at sizes between 4.5 nm and 80 nm, but the amounts are small. The main trend is that as the temperature increases, the major peaks shift to the lower diameters.

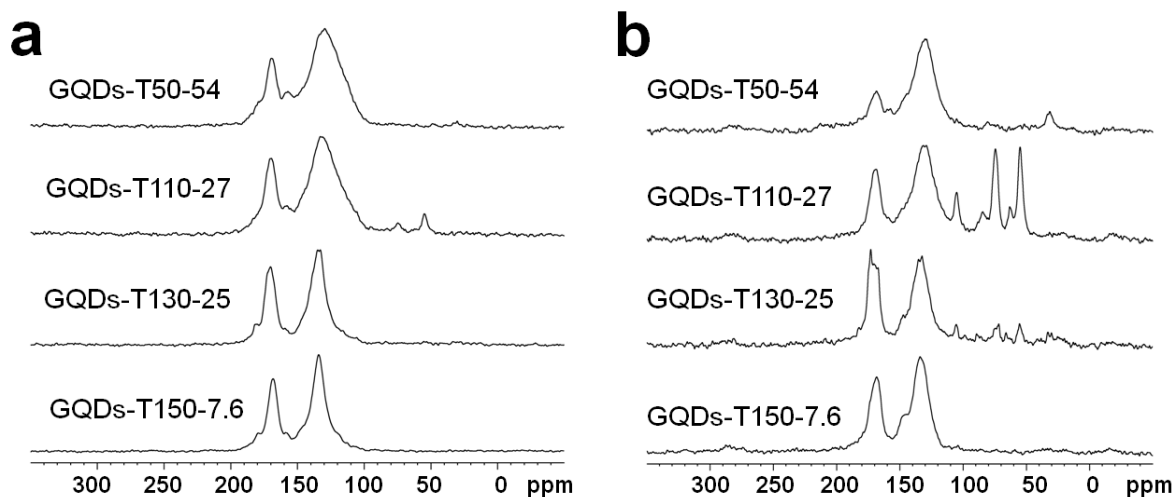


**Figure S8.** (a) Direct  $^{13}\text{C}$  pulse MAS NMR and (b) cross-polarization  $^{13}\text{C}$  MAS NMR spectra of

GQDs-T50-54, GQDs-T110-27, GQDs-T130-25 and GQDs-T150-7.6. The cross-polarization spectrum of GQD-T110-27 shows enhancement due to aliphatic impurities.

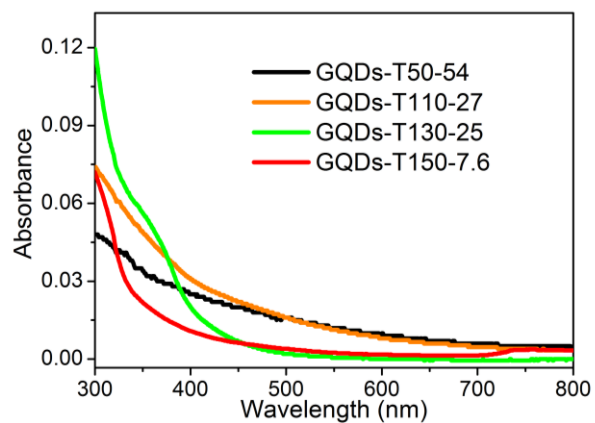


**Figure S9.** UV-Vis absorption of GQDs-T150-7.6, GQDs-T130-25, GQDs-T110-27 and GQDs-T50-54.

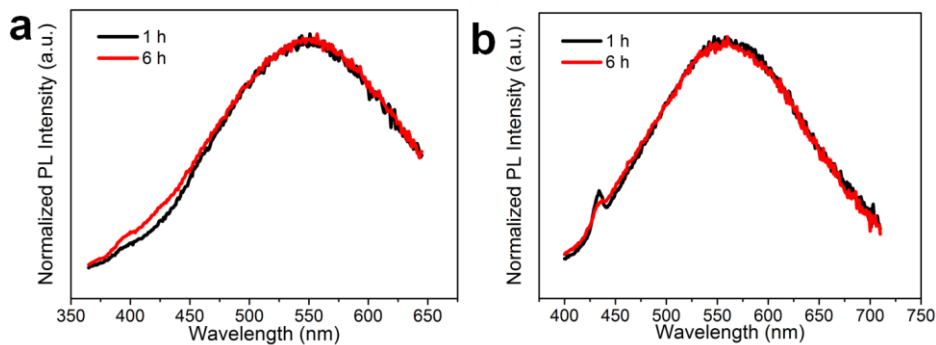


**Figure S10.** Emission spectra of GQDs synthesized at 130 °C for 1 h and 6 h. (a) Excited at 325 nm. (b) Excited at 365 nm.

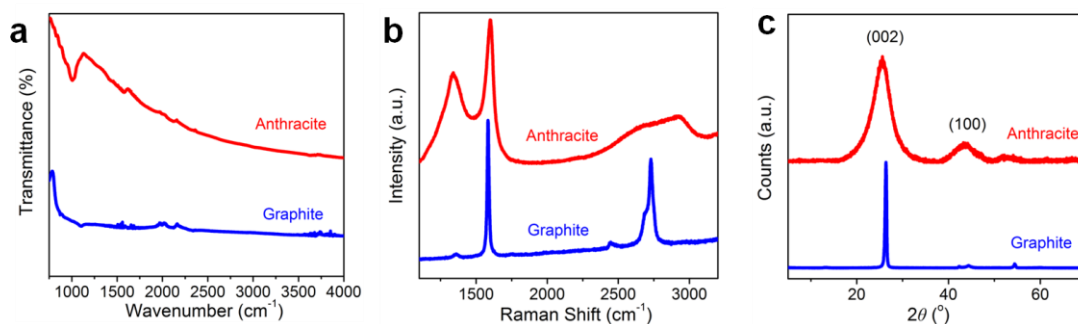


**Figure S11.** (a) FTIR (b) Raman and (c) XRD spectra of anthracite and graphite. In the Raman spectrum, the larger D peak at 1350 cm<sup>-1</sup> of anthracite indicates higher defect. In the XRD spectrum, the d-spacing for anthracite and graphite was 0.346 nm and 0.337 nm, respectively. The broader peak at ~26° for anthracite indicates a smaller crystalline domain.